Supplementary Information

In vivo recordings of brain activity using organic transistors

Dion Khodagholy[1], Thomas Doublet[1,2,3,4], Pascale Quilichini[2,3], Moshe Gurfinkel[1], Pierre Leleux[1,2,3,4], Antoine Ghestem[2,3], Esma Ismailova[1], Thierry Herve[4], Sébastien Sanaur[1], Christophe Bernard[2,3] & George G. Malliaras[1]

[1] Department of Bioelectronics, Ecole Nationale Supérieure des Mines, CMP-EMSE, MOC, 13541 Gardanne, France. [2] Aix Marseille Université, INS, 13005, Marseille, France. [3] Inserm, UMR_S 1106, 13005, Marseille, France. [4] Microvitae Technologies, Pôle d'Activité Y. Morandat, 13120 Gardanne, France. Correspondence should be addressed to G.G.M. (malliaras@emse.fr) or C.B. (Christophe.Bernard@univmed.fr).

Supplementary Figures

Supplementary Figure S1: Biocompatibility of PEDOT:PSS and parylene.

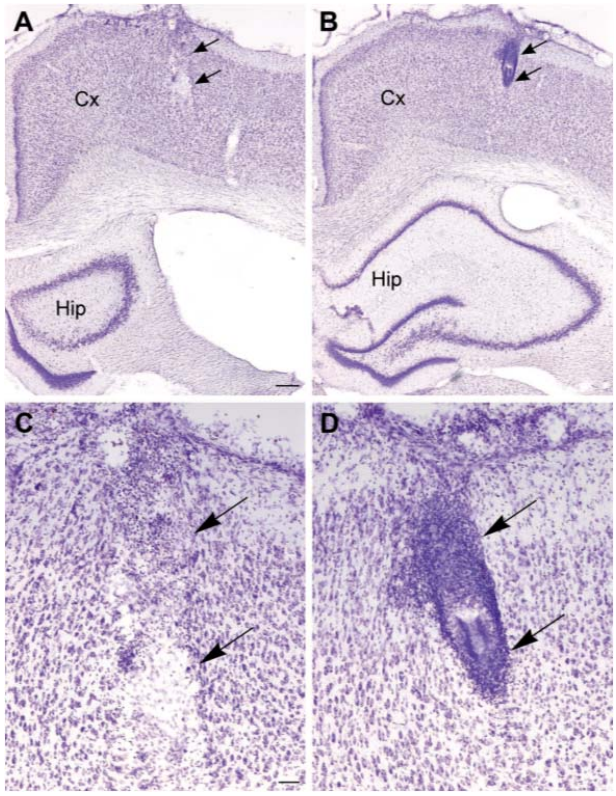

Comparison of histological profile induced by the parylene/PEDOT:PSS probe (A,C) and the silicon probe (B,D) implantation in the rat neocortex illustrated by sections stained with cresyl violet. Photomicrographs showing the tracks (arrows) of the parylene/PEDOT:PSS probe (A) and the silicon probe (B) implanted in a same rat, 1000 µm apart. At higher magnification, accumulation of glial staining is evident within the electrode tracks but does not extend to the surrounding tissue as illustrated by the presence of numerous healthy-looking neurons along the electrode tracks of the parylene/PEDOT:PSS probe (C) and the silicon probe (D). Note that the glial staining within the electrode track and cortical surface is less pronounced for the parylene/PEDOT:PSS probe than for the silicon probe, indicating a much better biocompatibility one month after implantation. Scale bars A, B: 250 µm; C, D: 50 µm. The arrows indicate the tracks of the probes and “Hip” stands for hippocampus.

Supplementary Figure S2: Frequency dependence of transconductance.

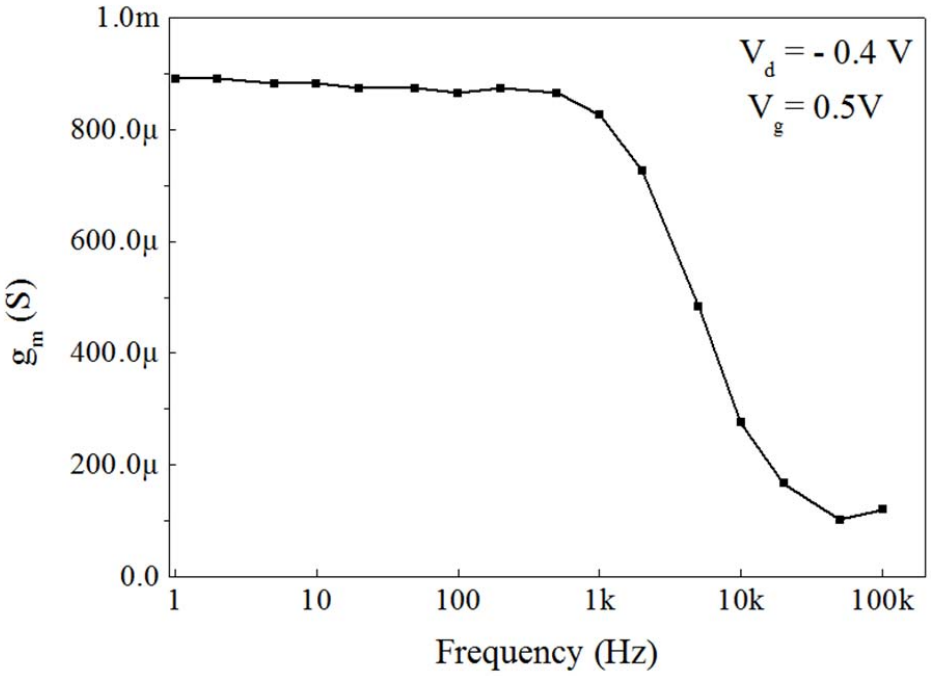

A low amplitude (50 $mV_{peak\text{-}peak}$) oscillation was added on a gate bias of 0.5 V and the small signal transconductance was determined by the amplitude ratio between the drain current oscillations and the corresponding input sine wave. The cutoff frequency (at which the transconductance drops by 3 dB from its plateau value) is approximately 5 kHz.

Supplementary Figure S3: Histogram of drain current of 32 OECTs fabricated on the same wafer.

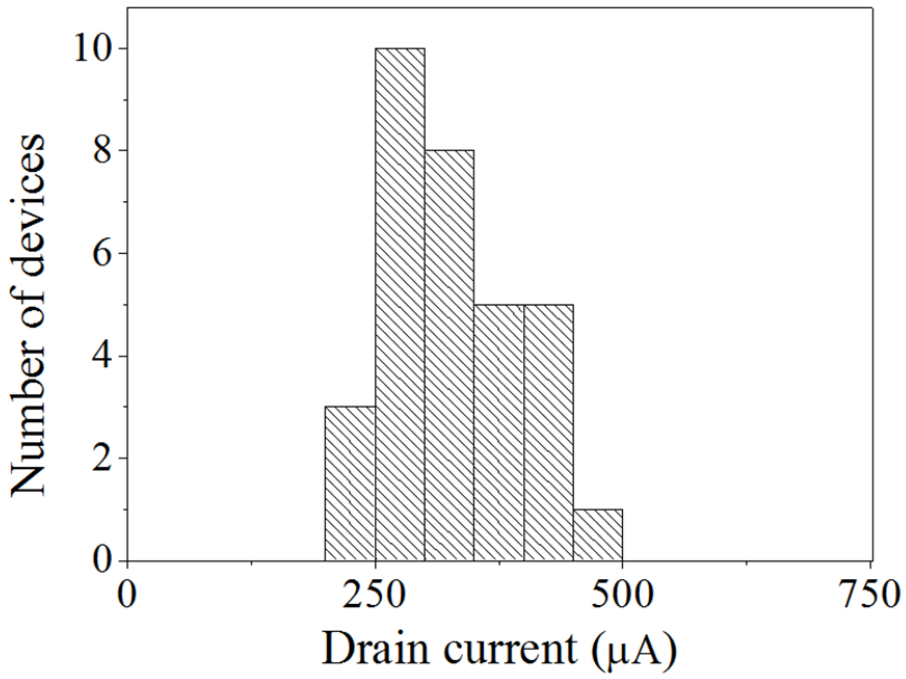

The yield was 100% (all devices worked as transistors). A Gaussian fit gave a mean drain current of 325.8 μA, with a standard deviation of 61.5 μA (V_d=-0.4 V, V_g=0 V).

Supplementary Figure S4: Results of OECT stability test over 8 hours.

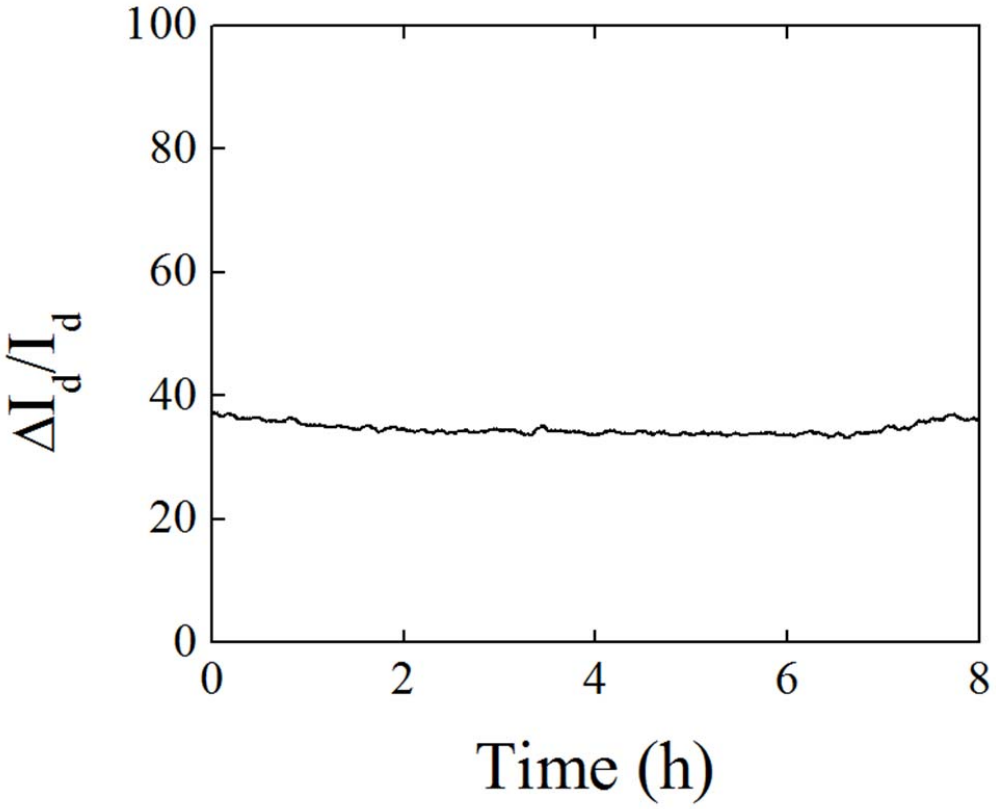

Relative modulation of the drain current (in %) of an OECT subject to repeated gate voltage pulses with an amplitude of 0.3 V, a duration of 10 s, and a duty cycle of 50% (V_d=-0.3 V). Phosphate buffered saline was used as the electrolyte.

Supplementary Figure S5: Results of OECT stability test over 5 weeks.

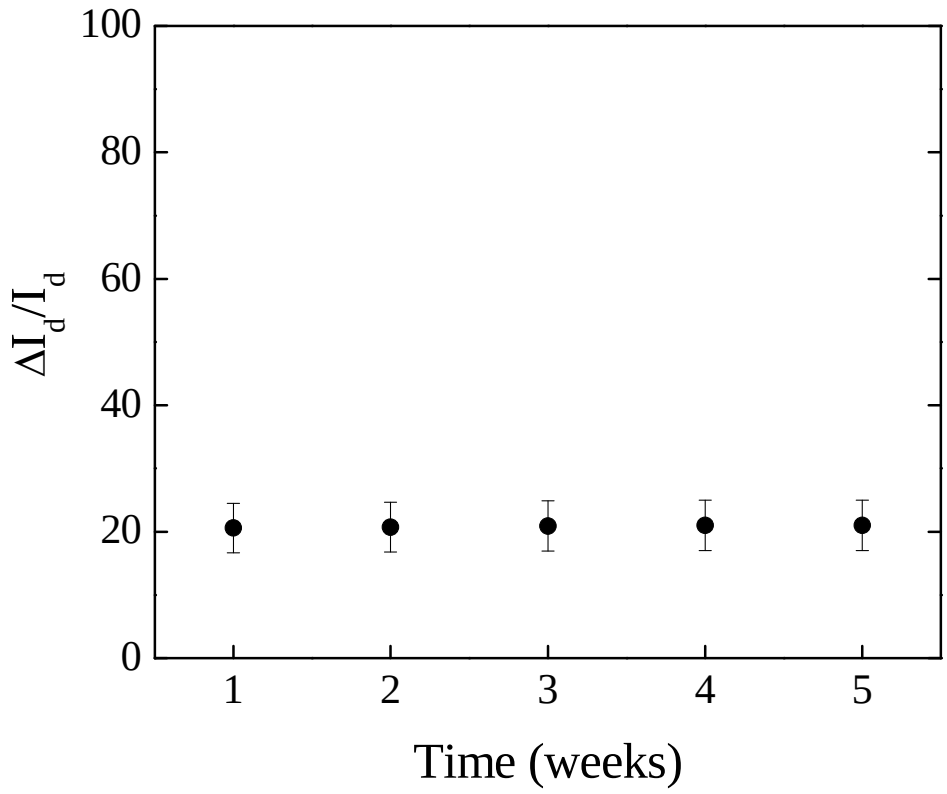

Relative modulation of the drain current (in %) of OECTs using DMEM complete cell culture media (Dulbecco) as the electrolyte and placed inside an incubator (37 ^{o}C). The modulation was measured once a week, using V_d=-0.3 V and V_g=0.2 V. In between the measurements the transistor was left unbiased. The error bars represent the standard deviation of data from 32 devices. Thanks are due to Dr. Leslie Jimison for supplying the data.

Supplementary Figure S6: Signal to noise ratio from power spectra.

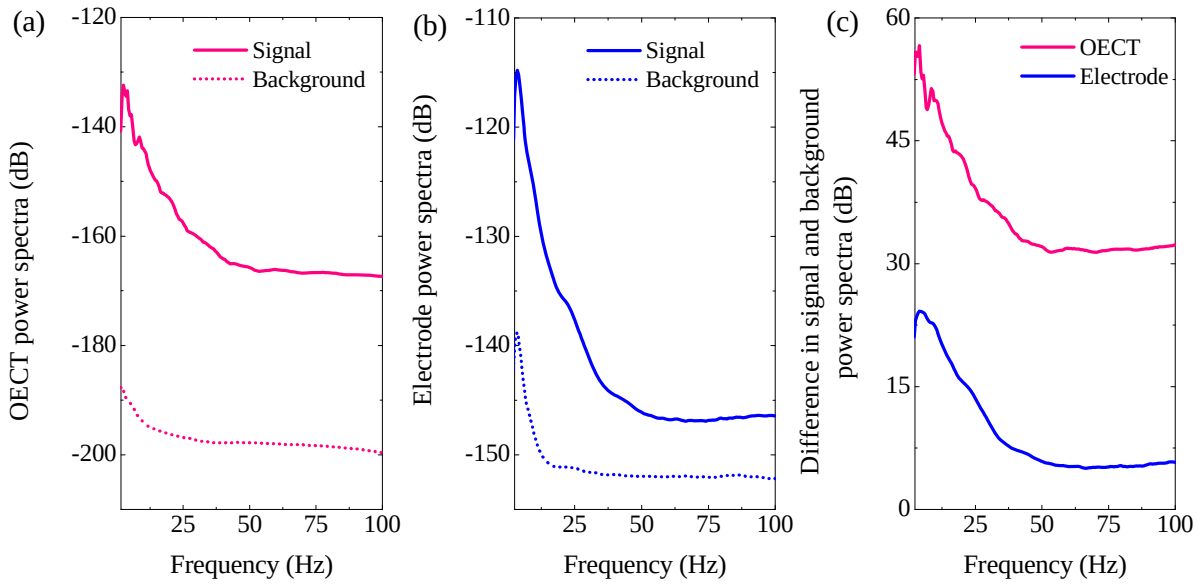

Power spectra of 30 seconds of recording during SWDs (signal) and of 30 seconds of recording during a period of low biological activity (background) made using the OECT (a) and the surface electrode (b). A Garbor wavelet with 0.5 Hz resolution was employed to achieve high temporal resolution of the non-stationary signals. The 50 Hz noise was removed by interpolating the power spectra to avoid any filtering artifacts. The difference in power of signal and background for the OECT and the surface electrode (c) shows that the transistor exhibits significantly higher power in the 0.5 – 100 Hz frequency range.